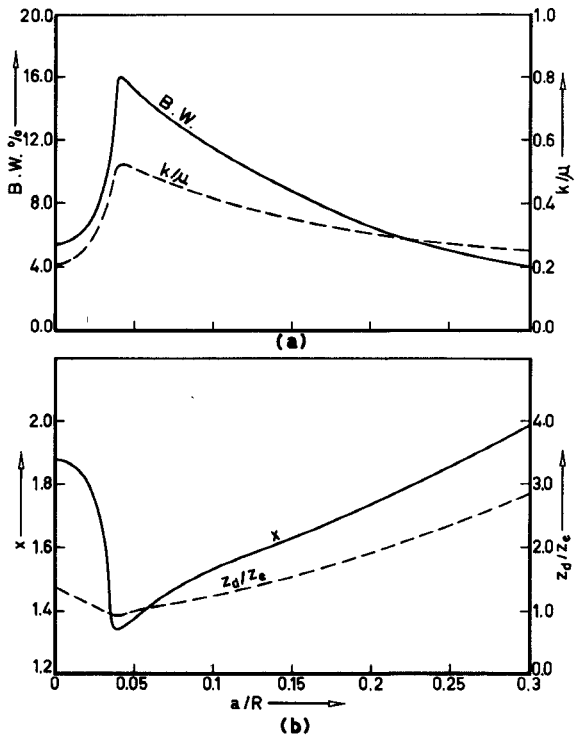

Fig. 3. The dependence of the maximum bandwidth and the corresponding values of k/μ, x, and Z_d/Z_e on the relative size of the metal post. $\psi = 18°$. (a) The maximum bandwidth and the ratio k/μ. (b) The normalized radius x and the impedance ratio Z_d/Z_e.

A compact broad-band stripline circulator can be realized using a 4-percent central metal post for $\psi = 18°$.

References

[1] C. G. Parsonson, S. R. Longley, and J. B. Davies, "The theoretical design of broadband 3-port waveguide circulators," *IEEE Trans. Microwave Theory Tech.* (Corresp.), vol. MTT-16, pp. 256–258, Apr. 1968.

[2] J. E. Pippin, "Ferrite-1968," *Microwave J.*, vol. 11, pp. 29–45, Apr. 1968.

[3] L. E. Davis, "Central pin tolerances in broadband 3-port waveguide circulators," *Electron. Lett.*, vol. 4, pp. 307–308, July 1968.

[4] J. B. Castillo and L. E. Davis, "Computer-aided design of three-port waveguide junction circulators," *IEEE Trans. Microwave Theory Tech.*, vol. MTT-18, pp. 25–34, Jan. 1970.

[5] J. W. Simon, "Broadband strip-transmission line Y-junction circulators," *IEEE Trans. Microwave Theory Tech.*, vol. MTT-13, pp. 335–345, May 1965.

[6] L. K. Anderson, "An analysis of broadband circulators with external tuning elements," *IEEE Trans. Microwave Theory Tech.*, vol. MTT-15, pp. 42–47, Jan. 1967.

[7] E. Schwartz, "Broadband matching of resonant circuits and circulators," *IEEE Trans. Microwave Theory Tech.*, vol. MTT-16, pp. 158–165, Mar. 1968.

[8] Y. Natio and N. Tanaka, "Broad-banding and changing operation frequency of circulators," *IEEE Trans. Microwave Theory Tech.*, vol. MTT-19, pp. 367–372, Apr. 1971.

[9] J. Helszajn, "Frequency response of quarter-wave coupled reciprocal stripline junction," *IEEE Trans. Microwave Theory Tech.*, vol. MTT-21, pp. 533–537, Aug. 1973.

[10] A. M. Hussein, M. M. Ibrahim, and S. E. Youssef, "Performance characteristics of 4-port stripline circulators," *IEEE Trans. Microwave Theory Tech.* (Short Papers), vol. MTT-23, pp. 923–926, Nov 1975.

[11] J. B. Davis and P. Cohen, "Theoretical design of symmetrical junction stripline circulators," *IEEE Trans. Microwave Theory Tech.*, vol. MTT-11, pp. 506–512, Nov. 1963.

[12] H. Bosma, "On stripline Y-circulation at UHF," *IEEE Trans. Microwave Theory Tech.*, vol. MTT-12, pp 61–72, Jan. 1964.

[13] H. Bosma, "Junction circulators," in *Advances in Microwaves*, vol. 6, L. Young, Ed. New York: Academic, 1971, p. 229.

[14] Y. S. Wu and F. J. Rosenbaum, "Wide-band operation of microstrip circulators," *IEEE Trans. Microwave Theory Tech.*, vol. MTT-22, pp. 849–856, Oct. 1974.

[15] F. J. Rosenbaum, "Integrated ferrimagnetic devices," in *Advances in Microwaves*, vol. 8, L. Young and H. Sobol, Eds. New York: Academic, 1974, pp. 263–282.

Full-Band Low-Loss Continuous Tracking Circulation in K Band

J. G. de KONING, MEMBER, IEEE,
R. J. HAMILTON, JR., MEMBER, IEEE, AND
T. L. HIERL

***Abstract*—The continuous tracking principle is applied to the design of a wide-band Y-junction stripline circulator for the 18–26.5-GHz frequency band. Near octave low-loss and high isolation performance is demonstrated without the need for repeated design cycles. Design data and construction details are presented.**

I. Introduction

In a recent paper [1], Wu and Rosenbaum discovered the continuous tracking technique for the design of octave bandwidth stripline and microstrip Y-junction circulators. By retaining terms up to the third order in the expressions for the electromagnetic fields, they obtained solutions for the perfect circulation roots and the intrinsic junction impedance ratio. This impedance ratio (Z_{eff}/Z_d) was found to be a nonmonotonic function of the anisotropic splitting ratio k/μ. It was further shown that by judicious choice of disk coupling half-angle, the intrinsic and external junction impedance ratios could be matched over the range $0.5 < k/\mu < 1.0$, thereby obtaining perfect circulation over a two-to-one frequency range. This continuous tracking technique was verified with a microstrip design. Moderately high isolation was found from 6.5 to 13 GHz, but the junction loss of approximately 1 dB was relatively high for a Y-junction circulator.

This short paper describes the application of the continuous tracking principle to the design of a wide-band stripline Y-junction circulator for the 18.0–26.5-GHz frequency band. High isolation as well as low loss have been obtained over the desired frequency range without the need for repeated design cycles. This indicates a high degree of both usefulness of the design principle and accuracy of the design procedure.

II. Wide-Band Circulator Design Procedure

Since the circulator described in this short paper is applied in the design of a low-noise Gunn-effect reflection amplifier, high isolation with minimum loss is required [2]. It was therefore decided, also in view of the high frequency of operation, to utilize balanced stripline construction. As a preliminary to the determination of the value of the coupling half-angle Ψ, which yields a matched impedance ratio over the widest possible frequency range, the following initial assumptions and material choices were made.

1) Assume a disk structure, implying

$$H_i = H_a - 4\pi M_s$$

where H_i is the internal magnetic field, H_a is the applied magnetic field, and $4\pi M_s$ is the saturation magnetization of the ferrite.

2) Set $H_i = 0$; therefore,

$$\omega_m/\omega = k/\mu$$

Manuscript received February 10, 1976; revised May 6, 1976. This work was sponsored by the Naval Electronics Laboratory Center, San Diego, CA, under the direction of J. Reindel.

J. G. de Koning was with the Solid State West Division, Varian Associates, Palo Alto, CA 94303. He is now with the Microwave Semiconductor Division, Hewlett Packard, Palo Alto, CA 94304.

R. J. Hamilton, Jr., and T. L. Hierl are with the Solid State West Division, Varian Associates. Palo Alto, CA 94303.

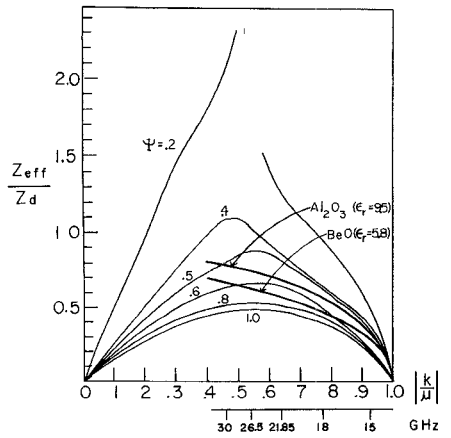

Fig. 1. Intrinsic junction impedance ratio as a function of anistropic splitting for various coupling angles (after Wu and Rosenbaum [1]), together with external junction impedance ratio for alumina and beryllia. (Operating frequency scale assumes a $4\pi M_s$ = 5000-G ferrite material with H_i = 0.)

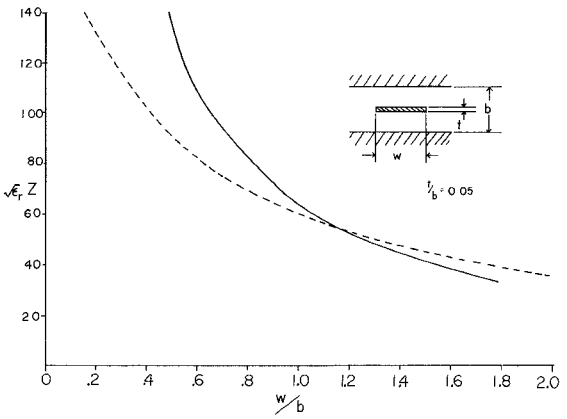

Fig. 2. Normalized stripline impedance versus w/b according to Cohn [4] (dashed curve). The normalized impedance to be maintained in order to avoid higher order modes is also plotted for the case w/b = 0.0152 in and a higher order mode cutoff frequency of 26.5 GHz (solid curve).

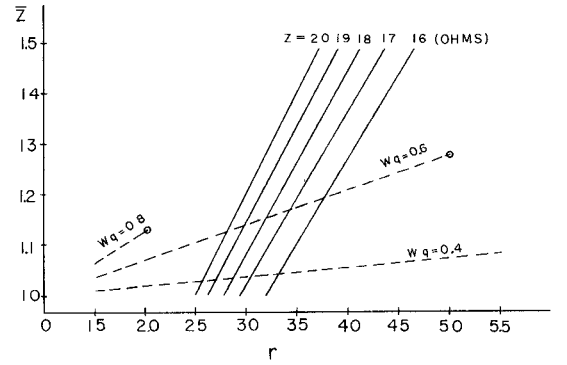

Fig. 3. Graphical aid for the determination of the transformer ratio of a three-section quarter-wave transformer with prescribed first step impedance Z.

where ω is the operating radian frequency $\omega_m = 2\pi \cdot \gamma \cdot 4\pi M_s$ and γ is 2.8 MHz/0e.

3) Use ferrite material with $4\pi M_s$ = 5000 G (Trans-Tech TT2-111).

4) Utilize a low-loss ceramic material such as alumina or beryllia for the matching structure.

The next step in the design procedure, in accordance with assumption 1), was to plot the external junction impedance ratio

$$Z_{eff}/Z_d = (\varepsilon_f/\varepsilon_d)^{1/2}(1 - (k/\mu)^2)^{1/2}$$

for alumina and beryllia, overlaying a plot of the intrinsic junction impedance ratio. In the preceding equation, ε_d and ε_f are the relative dielectric constants of the dielectric and ferrite, respectively. The result is shown in Fig. 1. A frequency scale is assigned to the horizontal axis in accordance with assumptions 2) and 3). Inspection of the figure reveals that close tracking can be achieved with alumina for Ψ = 0.57 rad over the desired frequency range. It was estimated using [1, fig. 5] that the propagation constant ferrite radius product SR was 1.48 at center band, and from this the ferrite radius was calculated to be 0.048 in.

Determination of Ground Plane Spacing and Matching Structure Design

In order to determine the ground plane spacing and design the matching structure, additional constraints and assumptions were as follows.

5) Only dominant mode propagation is allowed in the stripline matching structure [3].

6) Assuming that the junction is nonreactive, no reactive matching is required.[1]

7) Utilize a multisection quarter-wave matching transformer.

8) Adjust the ground plane spacing such that the first transformer step physically subtends an angle at the edge of the ferrite resonator equal to the coupling angle Ψ. This insures that the full potential bandwidth is realized [1].

In order to determine the maximum allowable ground plane spacing (b_{max}) in accordance with the restrictions imposed by items 5) and 8), Fig. 2 was constructed. The solid curve in the figure relates the stripline impedance to the maximum value of b for which only dominant TEM mode propagation exists up to 26.5 GHz for the conductor width w equal to 0.0512 in. This curve is based on calculations of the cutoff frequency of the first higher order TE mode and is, in fact, valid for any frequency band provided the ratio of the cutoff frequency to the center frequency remains a constant. The dashed curve shows the dependence of the actual impedance on w/b according to Cohn [4], and b_{max} can be derived from the minimum value of w/b which occurs at the intersection.

It may be seen from Fig. 2 that as long as w/b remains less than or equal to 1.138, mode-free operation is insured. In our case, w/b was chosen to be 1.137. The resulting ground plane spacing b was calculated to be 0.045 in. The corresponding impedance of the first transformer section was 18 Ω.

The last step in the design is to determine the impedance values of the remaining sections of the transformer.[2] This was accomplished by determining the value of the transformer ratio r utilizing Fig. 3. This ratio is found at the intersection of the solid curve marked 18 Ω which is the impedance of the first transformer step and the w_q (fractional bandwidth) = 0.6 line. The solid lines represent $\bar{Z}$ (the first step impedance normalized to the transformed impedance) as a function of the transformer ratio

[1] This assumption was based on the nonresonant nature of the continuous tracking approach but was not explicitly stated in [1]. The low VSWR (= 1.25:1) achieved in this work indicates that the junction at worst is only very slightly reactive.

[2] In [5, tables 6.02-2–6.02-5], it may be seen that a three-section transformer was required.

TABLE I

Ferrite material	TT2-111
$4\pi M_s$	5000 G
ε_f	12.5
H_a	5000 G
Dielectric material	AL 995 (WESGO)
ε_d	9.5
Ψ	0.57 rad
k/μ	0.64 at 21.85 GHz
SR	1.48 at 21.85 GHz
Ferrite diameter	0.095 in
Dielectric OD	0.271 in
Disk height	0.022 in
Number of transformer sections	3
Transformer ratio	3.33
Theoretical transformer bandwidth	0.6
Theoretical transformer VSWR	1.05

for various values of Z. The broken lines show dependence of $\bar{Z}$ upon r for w_q ranging from 0.4 to 0.6 for a three-section transformer. The curves are shown only for those values of r for which the VSWR remains below 1.05 [5]. It was found that a minimum of three sections was needed to obtain a transformer with wide enough bandwidth (0.6) and low enough VSWR (1.05:1). A suitable solution was found for a transformer ratio r of 3.33.

III. Mechanical Construction and Discussion of Performance Results

A summary of the design parameters and the major mechanical dimensions is given in Table I.

Ferrite cylinders were ground from TT2-111 bar stock and inserted with HYSOL adhesive in dielectric rings of AL 995 alumina. The center conductor was machined from brass and silver plated for low loss. The section of the transformer adjacent to the connector was realized in air stripline in order to allow alignment of the circulator by means of miniature tuning screws. The top and bottom ground planes of the ferrite resonator are formed by copper foil, the diameter of which equals that of the dielectric disk. The biasing magnetic field is generated by SmCo magnets, 0.25 in in diameter and 0.125 in high. These magnets were fabricated in our laboratories and fully charged and temperature stabilized. The biasing field in the gap in the absence of the disk was 5050 G. Miniature OSSM connectors were employed to circumvent higher order moding above 25.7 GHz encountered with SMA connectors. Fig. 4 shows a photograph of the miniature circulator with the top ground plane and top magnet removed. The overall size of the unit is 0.83 by 0.71 by 0.55 in excluding connectors. Fig. 5 represents insertion loss and isolation performance for all three ports of the circulator. Minor adjustment of the third step impedance was required to achieve this performance. A single-pass insertion loss of less than 0.5 dB was observed from 15.6 to 26.5 GHz. Isolation over the same range was approximately 20 dB minimum for all three ports. These performance levels continued to 27.0 GHz, resulting in a near octave fractional bandwidth of 56 percent. This bandwidth compares favorably with Wu and Rosenbaum's results. It is believed that the improved isolation and loss performance was partially due to the use of a balanced stripline medium and partially due to the use of a multisection impedance transformer.

Low-loss performance was maintained up to $|k/\mu| = 0.9$ which is into the range of $0.8 \leq |k/\mu| \leq 1.0$ where the magnetic loss tangent increases rapidly [6]. This performance is not clearly understood. The return loss at each of the ports was

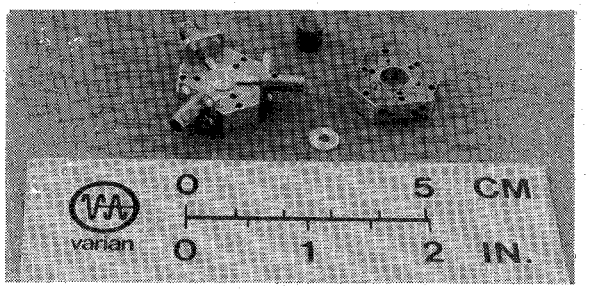

Fig. 4. K-band circulator with upper ground plane and upper ferrite resonator removed.

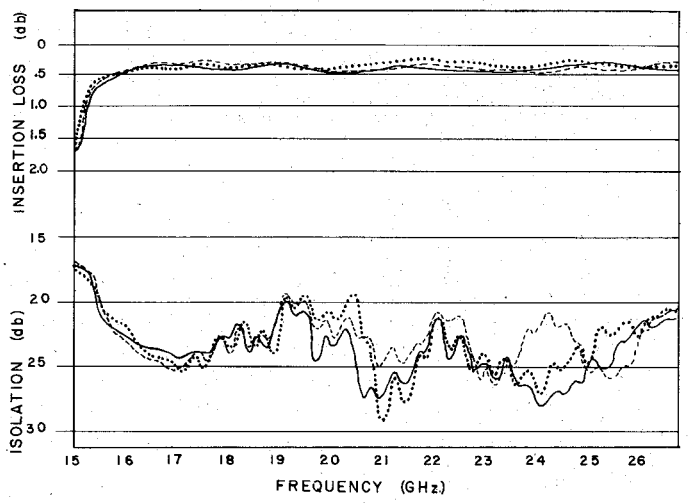

Fig. 5. Loss and isolation performance of K-band stripline junction circulator.

measured and maximum VSWR of 1.25:1 was calculated for all frequencies in the range of interest. The average VSWR was lower, being on the order of 1.15:1. As evidenced by the curves in Fig. 5, no sharp resonances or changes in VSWR usually associated with ferrite modes were found at any point in the band.

IV. Conclusion

It has been shown that the continuous tracking design approach can be advantageously employed for the design of near octave bandwidth stripline circulators in the 20-GHz region. A design procedure for the matching network has been proposed and demonstrated based on the nonresonant nature of the design principle. This procedure is generally applicable and graphs are presented for a specific cutoff frequency to center-band frequency ratio. It appears that this procedure sets an upper limit for the impedance of the transformer step adjacent to the ferrite, and that this upper limit is determined only by that ratio of frequencies mentioned previously.

Acknowledgment

The authors wish to thank G. Cirimele and R. Hendricks for their help in fabrication and assembly of the circulator.

References

[1] Y. S. Wu and F. J. Rosenbaum, "Wide band operation of microstrip circulators," *IEEE Trans. Microwave Theory Tech.*, vol. MTT-22, pp. 849–856, Oct. 1974.

[2] J. G. de Koning, R. E. Goldwasser, R. J. Hamilton, Jr., and F. E. Rosztoczy, "Fullband staggered gain Gunn effect amplification in *Ka*-band," *Proc. IEEE*, vol. 63, pp. 1371–1373, Sept. 1975.
[3] K. S. Packard, "Optimum impedance and dimension for strip transmission line," *IRE Trans. Microwave Theory Tech.*, vol. 5, pp. 244–247, Oct. 1957.
[4] S. B. Cohn, "Characteristic impedance of the shielded strip transmission line," *IRE Trans. Microwave Theory Tech.*, vol. MTT-2, pp. 52–57, July 1954.
[5] G. L. Mattheai, L. Young, and E. M. T. Jones, *Design of Microwave Filters, Impedance Matching Networks and Coupling Structures*. New York: McGraw-Hill, 1964, ch. 6.
[6] H. Bosma, "Junction circulators," in *Advances in Microwaves*, vol. 6. New York: Academic Press, 1971, p. 218.

Microwave Properties of Lithium Ferrites

JEROME J. GREEN, SENIOR MEMBER, IEEE, AND H. JERROLD VAN HOOK

***Abstract*—Low-power loss and high-power threshold properties have been measured between 3.0 and 17.2 GHz on three Li-Ti ferrite compositions of magnetizations 1250, 2250, and 3600 G. In each composition the use of cobalt resulted in a linear increase in μ_0'' and h_{crit}. Temperature measurements were performed at 9.2 GHz on the 2250-G material. An illustration of how the data might be applied is given.**

I. Introduction

In recent years the lithium–titanium system [1]–[2] has been a valuable addition to the microwave ferrite family. Through the use of titanium substitution, the magnetization can be conveniently varied between 0 and 3600 G (Fig. 1) while maintaining a high Curie temperature. Currently, the materials are made with small additions of bismuth and manganese [1]. The bismuth addition permits densification to greater than 99 percent of theoretical which is essential to achieve the low coercive force and high remanent magnetization necessary in phase shifter applications. Manganese is used to decrease the dielectric loss tangent to less than 10^{-3}. To improve peak power performance in spinels, it is traditional [3], [4] to add cobalt, and for high-average-power applications, where heating can be a serious concern, a low saturation magnetization is chosen. To achieve the lowest insertion loss and most compact device, one typically chooses the lowest cobalt level and highest saturation magnetization consistent with the peak and average power performance requirements. The choice of material is determined by the frequency of application, the peak and average power requirement, and the premium on weight and switching power. Therefore, it is desirable to know the material parameters which affect device performance of a wide variety of compositions to be able to perform the necessary tradeoffs in selecting a specific composition.

In this paper we describe the microwave properties of three basic lithium–titanium compositions which have room temperature saturation magnetizations of 1250, 2250, and 3600 G. This range of magnetizations covers applications between 5.5 to 17.0 GHz. The chemical formula for these compositions is

$$Li_{0.5+(x/2)-(z/2)}Mn_yTi_xCo_zFe_{2.5-(3x/2)-y-(z/2)}O_4$$

Manuscript received December 1, 1975; revised May 25, 1976. This work was supported in part by the U.S. Air Force Materials Laboratory, Wright-Patterson Air Force Base, under Contract F33615-72-C-1524.
The authors are with the Raytheon Research Division, Waltham, MA 02154.

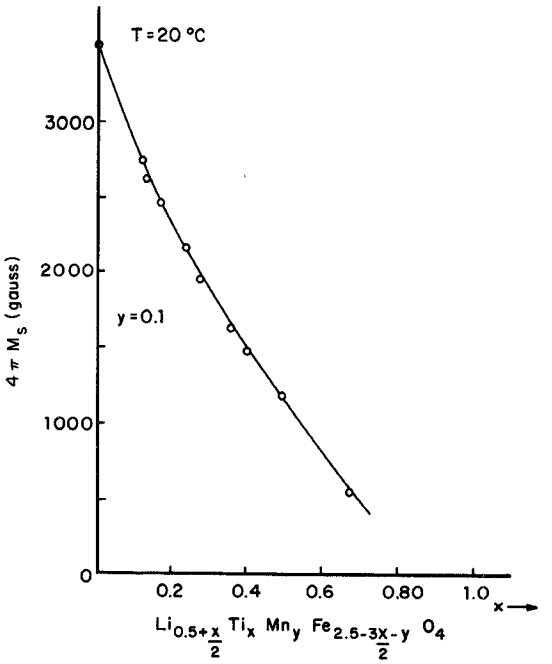

Fig. 1. Saturation magnetization versus titanium content at 20°C.

where $x = 0$ for $4\pi M_s = 3600$ G, $x = 0.26$ for $4\pi M_s = 2250$ G, and $x = 0.53$ for $4\pi M_s = 1250$ G. The Mn level in all compositions was kept at $y = 0.1$. The range in Co concentration was between $0 \leq z \leq 0.04$. Bismuth oxide (Bi_2O_3) is added at low concentrations in the original formulation of the ferrite, the purpose being to promote densification and grain growth [1] in the final sintering step. Concentrations in the range of 0.1 to 0.2 weight percent of the original batch are generally used. The Bi_2O_3 addition is essentially insoluble in the ferrite, residing primarily in boundary regions between ferrite grains where its influence on sintering kinetics is strongest. We have therefore not included Bi_2O_3 in the chemical formulation of the ferrite.

The magnetic loss parameter μ_0'' and peak power parameter h_{crit} of these three compositions has been evaluated primarily in the vicinity of 5.5, 9.2, and 17.0 GHz. Some microwave measurements were made as a function of temperature at 9.2 GHz. The experimental techniques were similar to those used for our previous papers [5], [6].

II. Temperature Dependence of Magnetization and Coercive Force

The temperature dependence of a phase shifter's differential phase shift and insertion phase is determined by the temperature performance of the hysteresis loop properties. Fig. 2 gives the dependence of the saturation magnetization upon temperature T, and Figs. 3–5 show the dependence of the remanent magnetization $4\pi M_r$ and coercive force H_c upon T. For high cobalt content there is a decrease in remanence at low temperature for the 1250- and 3600-G materials. This decrease in remanence has been previously described by Van Hook and Dionne [7] for the 3600-G composition. It is suggested that the effect is due to a change in sign of the anisotropy constant K_1 [8]. For the 1250- and 2250-G composition it has not been possible to grow single crystals so that we do not know how the anisotropy constant K_1 depends upon Co content and temperature in these compositions. We can only speculate that the same mechanism is at work in the